Journal of Modern Trends in Physics Research
Online ISSN 2636-4220
DOI: 10.19138/mtpr/(16)1-10
Accepted: 2016-12-20

Detection of interplanetary coronal mass ejections' signature using artificial neural networks

Ramy Mawad[1,2,*], A. Radi[3,2], R. Saber[2,4], A. Mahrous[2,5], Mohamed Youssef[2,5], Walid Abdel-Sattar[6], Hussein M. Farid[6], Shahinaz Yousef[6]

[1] *Astronomy and Meteorology Department, Faculty of Science, Al-Azhar University, Nasr City, Cairo 11488, Egypt.*
[2] *Space Weather Monitoring Center, Helwan University, Ain Helwan, Egypt.*
[3] *Physics Department, Faculty of Science, Ain Shams University, Cairo, Egypt.*
[4] *Physics Department, Obor Academy, Cairo, Egypt.*
[5] *Physics Department, Faculty of Science, Helwan University, Ain Helwan, Helwan 11795, Egypt.*
[6] *Astronomy, Space Science & Meteorology Department, Faculty of Science, Cairo University, Giza 12613, Egypt.*

* Corresponding author (Email: ramy@azhar.edu.eg)

Abstract- We have estimated the arrival time of interplanetary coronal mass ejection (ICME) shocks during solar cycle 23 (the period from 1996 to 2007) using the artificial neural network. Under our model, we could match 97% of the listed coronal mass ejection CME-ICME events selected by [Cane and Richardson (2010)] using the initial velocities of the ICME events. Whereas, when we used the ICME velocity at a distance $20R_{\odot}$, our model succeeded to match only 84% of the listed ICME events. The prediction of CME travel-time correlated to the initial speed of CMEs, we found a high correlation coefficient between initial speed of CME and calculated travel time under our model ($R \approx 74$) with power fitting. The prediction of ICME arrival time can be better estimated from initial speed and linear speed of CMEs more than from final speed or speed at 20 $R_{\odot}$.

Keywords- Space Weather; Coronal Mass Ejection; Interplanetary Coronal Mass Ejection; CME; ICME; ICME shock; CME Travel Time; ICME Arrival Time.

1. INTRODUCTION

The prediction and effects of solar activity on the terrestrial environment on long periods are of great interest since the beginning of the 20th century [Forbush (1938), Duperier (1942)]. This is a branch of physics called "Solar terrestrial connection". The prediction of solar activity through short periods is called "space weather", while prediction of solar activity through days is called "space physics". Space weather is the study of the impact of solar activity's phenomena and its prediction through days on the terrestrial environment, such as their relationship with sunspots, solar flares, solar filaments and prominence, solar wind, coronal holes, Coronal Mass Ejections (CMEs), or even Interplanetary Coronal Mass Ejections (ICMEs), interplanetary shocks, and magnetic clouds (MC) or interaction regions, which also affects planetary atmospheres and dynamics, was not established until the first space missions with appropriate in-situ instrumentation.

When solar activity reaches the earth's atmosphere, important events could be triggered all around the planet and can even change the atmospheric composition [Low (2001)], magnetospheres' altitude [Mawad *et.al.* (2014b)] and temperature [Gardner *et al.* (2012); Clausen *et al.* (2014); Mawad (2015)]. In consequence, it changes Earth's orbit, causing perturbation [Mawad, (2015)], and lowering of satellites' orbits too.

The strongest geomagnetic disturbances are caused mainly by solar plasma (such as CMEs) traveling towards Earth. Because of destructive effects of space weather on space and ground-based technical systems (e.g. spacecraft charging, lowering of orbit, communication interruptions, flow of induced currents along transmission lines), making the prediction of the arrival time of a CME at 1AU, and its properties at that time, highly desirable [Owens and Cargill (2004)].

CMEs are known to be the major cause of severe geomagnetic disturbances, often referred to as space weather. These CMEs can affect Earth's magnetosphere's environment and technological systems [Gopalswamy *et al.* (2001)].

CME is the most important source of space weather. The prediction of the solar plasma's arrival time clouds such

Journal of. Modern Trends in Physics Research
Online ISSN 2636-4220
DOI: 10.19138/mtpr/(16)1-10
Accepted: 2016-12-20

as ICME to the 1 AU from the Sun (near to Earth) has been studied by several of researches.

The present generation of forecasting models all predict the travel time of a CME to 1AU, this time is defined as being the time between the first observation of the CME by a coronagraph, and the arrival of the leading edge of the ICME at 1AU [Owens and Cargill (2004)]. According to McKenna-Lawlor et al. (2002), the arrival times at the Earth of eleven flare associated halo CMEs generated shocks, for the period (1997-2001), were forecasted based on "real-time" data using three numerical models, namely the Shock Time of Arrival Model (STOA), the Interplanetary Shock Propagation Model (ISPM) and the Hakamada-Akasofu-Fry Solar Wind Model (HAFv.2). These predictions are compared with the measured arrival times. The models are all generally successful in predicting shock arrivals. STOA scored the smallest values of "predicted minus observed" arrival times (typical precision better than 8 h). The ratio of the calculated standard deviation of the transit times to Earth to the standard deviation of the measurements was estimated (treating interacting events as composite shocks) for each model and these ratios turned out to be 0.60, 1.15 and 1.02 for STOA, ISPM and HAFv.2, models respectively.

More than 70% of geomagnetic storms are caused by ICMEs arriving at Earth [Zhang *et al.* (2007)]. An ICME is the solar wind counterpart of a CME. This solar ejection drives a well-developed interplanetary shock, and a well-defined magnetic structure named the MC occasionally transported by ICMEs to Earth's orbit [Richardson and Cane (2011)]. MCs are structures observed in the solar wind that are characterized by a smooth magnetic field rotation, a relatively high magnetic field intensity, and a relatively low temperature [Burlaga *et al.* (1981)]. These MCs were once detected in one-third of the ICMEs, although this frequency likely depends on the ICME region through which Earth is traversing [Hidalgo *et al.* (2013)].

Interplanetary coronal mass ejections (ICMEs) are understood to be the Heliospheric counterparts of CMEs, with signatures undeniably linked to the CME process, the variability of these signatures and questions about the features of observed CME raise issues that remain on the cutting edge of ICME research. These issues are discussed in the perspective of traditional understanding, and recent results using innovative analysis techniques [Wimmer-Schweingruber *et al.* (2003)].

The heliospheric counterparts of coronal mass ejections (CMEs) at the Sun, interplanetary `coronal mass ejections (ICMEs), can be identified in situ based on a number of magnetic fields, plasma, compositional and energetic particle signatures as well as their combinations. Zurbuchen and Richardson (2006) summarize these signatures and their implications for understanding the nature of these structures and the physical properties of coronal mass ejections, they state that our understanding of ICMEs is incomplete and face several challenges that, if well studied, would significantly improve our knowledge of the relationship between CMEs at the Sun and in the heliosphere.

Fast ICMEs will tend to drive a shock, which is not a signature of the ICME proper, but, a convenient, often used and reasonably well-understood signature associated with many ICMEs. This shock can accelerate particles. The turbulence in the sheath following the shock modulates their propagation and is an important ingredient in the acceleration process. However, it is sometimes difficult to identify the boundary between the ICME and the trailing edge of the sheath. This may be due partly to the dynamic nature of ICME propagation, and possibly to evolve with time, e. g., by reconnection [e. g., Cargill and Schmidt (2002); Gosling *et al.* (2005)].

Moreover, different in-situ signatures do not necessarily give the same boundaries. The ICMEs' internal structure can be highly inhomogeneous, which will cause difficulties in identifying substructures and boundaries with different signatures.

The geomagnetic disturbance is the main indication of arrival of ICME to Earth (1 AU). Some of researchers used SSC as an indication of arrival time of ICME (at 1 AU) and paired it with CME (at the Sun) to modeling travel time of CME-ICME [Shaltout *et al.* (2008), Mawad and Shaltout (2011); Mawad et al, (2014a)]. Using numerical simulation, Whang and Burlaga (1981) investigated the interactions of interplanetary shock waves beyond 1 AU. Their result showed that when a forward and a reverse fast shock propagate toward each other and collide, both shocks individually are limited.

Gopalswamy *et al.* (2000 & 2001) and Michalek *et al.* (2004) in their work established an empirical model to predict 1-AU arrival time of the CMEs. Gopalswamy *et al.* (2000) model could not account for the observation that CMEs with a slow initial speed (U <500 km/s) have an approximately constant travel time of 4.2 days. So a modification has been done for that model by assuming that ICME acceleration ceased at 0.76 AU (d1) for all CMEs (found to be the best fit), regardless of their initial speed, so the total travel time of the CME from the sun to 1 AU is the sum of the travel time to d1 at constant acceleration, and the travel time taken from d1 to 1AU: (d2=1AU-d1) at constant speed [Gopalswamy *et al.* (2001)]. Their model was based on the fact that the speed distribution of ICMEs, detected by the

Journal of. Modern Trends in Physics Research
Online ISSN 2636-4220
DOI: 10.19138/mtpr/(16)1-10
Accepted: 2016-12-20

Wind spacecraft was narrow (range 300–1000 km/s) compared to the velocity distribution of CMEs observed by SOHO/LASCO near the sun (100–2000 km/s). CMEs are ejected and accelerated by the magnetic field of the corona in the interplanetary space according to their relative velocities with the solar wind. ICMEs are depending on their speed relative to the solar wind, either accelerated or decelerated towards the solar wind speed. Fast CMEs are decelerated mostly by the solar wind due to friction which is proportional to the square of the velocity difference [Michalek *et al.* (2004)]. Gopalswamy et al. (2001) studied 47 events through the period (1996-2000) and obtained a mean time error about 10.7 hours.

A list of near-Earth interplanetary coronal mass ejections was compiled to be the interplanetary manifestations of the coronal mass ejections seen near the Sun by coronagraphs [Richardson (1997)].

To ensure that a CME and ICME are manifestations of the same ejection from the sun (and are not subject to strong interaction with other ejections), it is required that an observation of a single halo CME be followed 1 to 5 days later by a clear ICME signature in the magnetic and plasma data at 1AU. However, such ideal situations are quite rare around Solar Maximum. Owens and Cargill (2004) relaxed the selection criteria in order to have enough CME-ICME pairs for comparison with models. Richardson and Cane (2008) introduced a list of near-Earth interplanetary coronal mass ejections, which are believed to be the interplanetary manifestations of the coronal mass ejections seen near the sun by coronagraphs. They studied the effects of ICMEs on energetic particles, including those accelerated by solar flares, interplanetary shocks, and galactic cosmic rays, during 1996-2002. To examine these effects; it is needed to know when ICMEs are passing the observing spacecraft. Conversely, energetic particle observations can help to indicate when ICMEs are present. Some two dozen in-situ signatures of ICMEs (earlier terms include "shock drivers", "pistons", "ejecta") have been reported in magnetic field, plasma, solar wind composition and charge states as well as energetic particles from super thermal solar wind to galactic cosmic ray energies [Zurbuchen and Richardson (2006)]. Thus, ideally, ICME identification should combine as many data sets as possible, such as those available from ACE and other near-Earth space crafts.

The characteristics of magnetic clouds are enhanced when the magnetic field is greater than 10 nT and is varying gradually low proton's temperature and low plasma's beta [Klein and Burlaga (1982); Lepping *et al.* (1990)].

Cane and Richardson (2010) revised catalog of about 300 near-Earth ICMEs in the period 1996-2009, covering the complete cycle 23, and summarize their basic properties and geomagnetic effects. Their additional data confirm the earlier identifications based primarily on other solar wind plasma and magnetic field parameters. However, the boundaries of ICME-like plasma based on charge composition data may deviate significantly from those based on conventional plasma/magnetic field parameters.

2. OBJECTIVES

Our research aims to examine the ability to use ANNs to list the CME-ICME and compare them with other manually and empirically listed events. Besides, we check for the right velocity choice to be used in future numerical prediction. We used the list of Richardson and Cane ICMEs in 1996-2007 to construct our neural model.

3. ALTERNATIVE METHOD: ARTIFICIAL INTELLIGENCE

The detection of ICME's signature and solar wind empirically and numerically are so difficult. Hence, automatic detection is very difficult. Programmatically, there is a high diversion from manual selection of ICME. Traditional models in this field have been developed in the form of regression and time series models or some conceptual ones. The artificial intelligence is the best choice when mathematics fails. Artificial Neural Networks (ANNs) are going to be the best alternative for the previous empirical models. An attractive feature of ANNs is their ability to extract the relation between the inputs and outputs of a process, without physics being explicitly provided [ASCE (2000)].

Vandegriff *et. al.* (2005) used ANNs to predict the time remained to the interplanetary shock arrival. This algorithm was able to forecast the arrival time for 19 previously unseen events, after training on only 37 events.

The average uncertainty in the prediction (24 h in advance) was 8.9 h, while the uncertainty improved to 4.6 h when the event was 12 h away.

We used many numerical algorithms to list the ICME from their signature programmatically, but without successful results, it gives poor selections than manual selections. The problem depends on CME velocity choice (initial, linear, final and at $20R_{\odot}$) and no tracing for CMEs movement from eject time from the sun to near-earth arrival time. ICME may interact with space such as solar wind; the selection becomes difficult when Sun is active, whereas the solar wind

Journal of. Modern Trends in Physics Research
Online ISSN 2636-4220
DOI: 10.19138/mtpr/(16)1-10
Accepted: 2016-12-20

signatures become complex overlapping.

3.1. *Artificial Neural Networks (ANNs)*

An artificial neural network is made up of many simple and highly interconnected computational elements [Bhat *et. al.* (1990); Bourquin *et. al.* (1997)], which are called artificial neurons or nodes (Figure 1). These nodes are distributed on many different layers: one input layer, one or many hidden layers and one output layer. The nodes in adjacent layers are fully or partially interconnected with weighted links. The net input into the j^{th} layer node ($in[j]$) is equal to the sum of weighted outputs from the prior i^{th} layer ($out[i]$).

$$in[j] = \sum w_{ij} out[i] \qquad (1)$$

where, w_{ij} is the weight factor.

The hidden neurons (neurons of the hidden layers) and the weight factors of the links between them play a critical role during the learning process. In the case of supervised training, the numerical values of the weight factors change according to the training data sets, in order to minimize the difference between the actual outputs and the target value. Thus, the relationship between causal factors and response is mapped during the learning process.

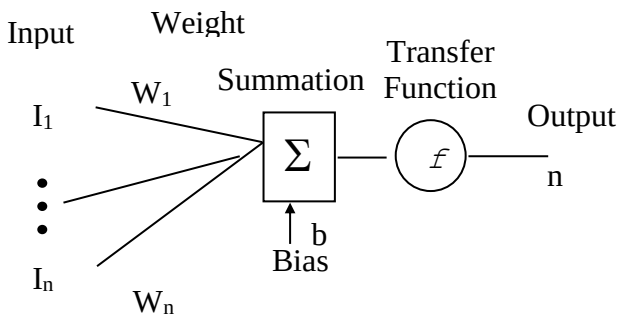

Figure 1: Neuron Model.

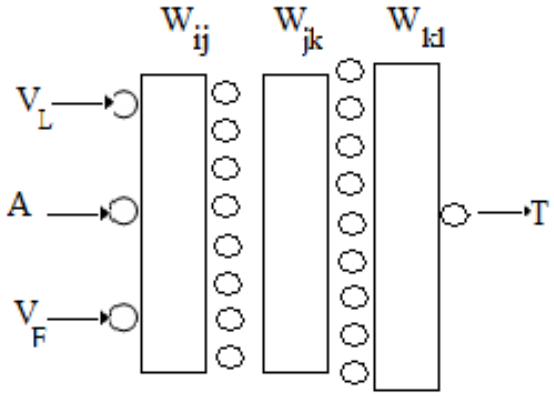

Figure 2: The A-A NN based modeling.

The transfer function of processing nodes is used to determine the output value of the node based on the total net input from nodes in the prior layer. The most widely used transfer function is a sigmoid function, which is shown in the following equation:

$$out[j] = \frac{1}{1 + e^{-in[j]}} \qquad (2)$$

Where $in[j]$ is the sum of the net inputs from nodes of the prior layer and $out[j]$ is the output from the j^{th} hidden layer node.

Inputs to neurons could be either from external stimuli or from the outputs of neurons from prior layers. Single outputs from neurons could be inputs to many other neurons in the network. When the inputs of the neuron exceed a certain threshold, specified by a threshold (transfer) function with bias, the neuron is fired, and an output signal is produced. When the weights are tuned via the learning process, the network recognizes the input-output relation (mapping function) .The number of nodes in the input layer is determined by the number of independent variables to be investigated. The number of nodes in the output layer is determined by the number of dependent variables. The number of hidden layers and the number of hidden nodes in each layer is strongly dependent on the complexity of the problem [Baum and Haussler (1989); Looney (1996)]. The optimal number of hidden nodes depends on many factors such as the number of input and output nodes, the number of training data sets, the amount of noise in the targets and

Journal of. Modern Trends in Physics Research
Online ISSN 2636-4220
DOI: 10.19138/mtpr/(16)1-10
Accepted: 2016-12-20

the complexity of the function or classification to be learned. There is no magic formula to use, to determine the number of hidden layers, and the number of nodes in each layer. Trial and error approaches remain the most commonly used methods; however, some rules of thumb and empirical formulas may be used as guidance.

3.2. *ANN Modeling*

The proposed ANN model has three inputs and one output. The inputs are the linear velocity (VL), the final velocity (VF) and the acceleration (A). The output is the time (T) Using this input-output arrangement, different network configurations were tried to achieve good mean sum square (MSE) and good performance for the network. The configuration, shown in figure 2, was chosen. It consists of an input layer 3 neurons, two hidden layers of 8 and 9 neurons, respectively, and an output layer one neuron. The transfer functions were chosen to be a log sigmoid function for the first and the second hidden layers and a linear sigmoid function for the output layer.

3.3. *Training of the A-A-ANN*

Training an ANN consists of making a particular input leads to a specific target output. The weights are adjusted, based on a comparison of the output and the target, until the network output gets as close as possible the target value. The proposed ANN model was trained using Levenberg-Marquardt optimization technique [Hagan and Benhaj (1994); Hamid (1998)]. This optimization technique is more powerful than the conventional gradient descent techniques. The Levenberg-Marquardt updates the network weights using the following rule:

$$\Delta W = (\mathrm{J}^{\mathrm{T}}\ \mathrm{J} + \mu\ \mathrm{I})^{-1} J^{T} e \qquad (3)$$

Where J is the Jacobean matrix of derivatives of each error for each weight μ is a scalar, changed adaptively by the algorithm and e is an error vector. The linear training weight was also chosen using the Nguyen-Widrow random generator to speed up the training process.

Collected data from experiments are divided into two sets, namely, the training set and validation set. The training set is used to train the ANN model by adjusting the link weights of the network model, which should include the data covering the entire experimental space. This means that the training data set must be fairly large to contain all the required information and must include a wide variety of data from different experimental conditions, including different formulation composition and process parameters.

Linearly, the training error keeps dropping. If the error stops decreasing or starts to rise, the ANN model starts to over-fit the data, and at this point, the training must be stopped. In case over-fitting or over-learning occurs during the training process, it is usually advisable to decrease the number of hidden units and/or hidden layers. In contrast, if the network is not sufficiently powerful to model the underlying function, over-learning is not likely to occur, and the training errors will drop to a satisfactory level. Therefore, the training data can be used to check the architecture and training progress of the ANN model.

The validation data set is used to confirm the accuracy of the ANN model. It ensures that the relationship between inputs and outputs, based on the training and test sets are real, and not artifacts of the training process. The validation data set should include data, which are not included in the training data set, but lie in the data boundaries of the training data set.

4. DATASET

We used the near-Earth ICMEs during the period 1996-2007 listed by Cane and Richardson. The data obtained from URL: http://www.srl.caltech.edu/ACE/ASC/DATA/level3/icmetable2.htm

We used the solar wind data observed by OMNI satellite, from at Space Physics Data Facility (SPDF).

5. RESULT AND DISCUSSION

Detection of ICME Signature

The upper panel of figure 3 shows the 3-dimensional dependence of the initial ICME velocity on both corresponding

Journal of. Modern Trends in Physics Research
Online ISSN 2636-4220
DOI: 10.19138/mtpr/(16)1-10
Accepted: 2016-12-20

travel time and acceleration. Whereas the lower panel demonstrates 3-dimensional reliance of the ICME velocity at $20R_{\odot}$ on both corresponding travels time and acceleration. The dot events (·) represent the Cane and Richardson listed travel time. While the circle events (○) stand for our neural model calculated travel time.

By examining the upper panel of figure 3, it is easy to notice that 97% of the dot ICME events coincided with the circle events. This means that our model succeeded to predict 97% of the Richardson and Cane listed ICMEs if we use the initial ICME velocity in our calculations. While, the lower panel demonstrated that for using the ICME velocity at 20 $R_{\odot}$ in our calculations, our model matched only 84% of the Richardson and Cane listed ICME events. The prediction result of the initial velocity of CME is better than that of the CME velocity at 20 $R_{\odot}$ because the initial velocities of CME are near the actual values since there is no interaction with the solar wind. Whereas, as the CME moved a distance 20 $R_{\odot}$ from the solar surface an interaction occurred with the solar plasma so the CME velocity at 20 $R_{\odot}$ is not actual but relative with the solar wind. Besides, this can be explained as the initial speed is obtained from the initial fitting of the ICME height-time relationship, while the ICME $20R_{\odot}$ speed is obtained from the second-order fit.

We found a high correlation between calculated travel times with initial speeds, correlation coefficient R≈74 with power fitting (figure 4). Also, we plot the travel time with speed at $20R_{\odot}$ (figure 5), final (figure 6) and linear (figure 7), the values are 74, 60, 63 and 72 respectively. The linear speed is acceptable; it gives a good correlation near to initial speed with detection's Neural Networks. The CME acceleration decrease with speed increase as shown in figure 8, the correlation coefficient R≈0.55 with linear fitting.

The prediction of ICME arrival time can be better estimated from initial speed of CME, the linear speed is acceptable too.

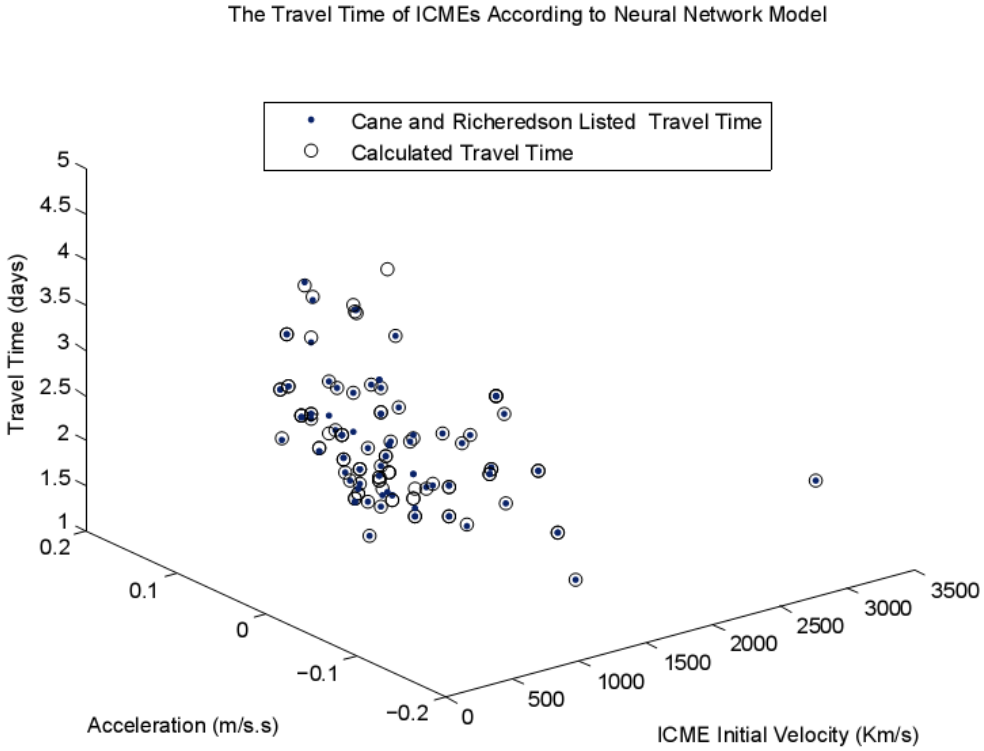

Journal of. Modern Trends in Physics Research
Online ISSN 2636-4220
DOI: 10.19138/mtpr/(16)1-10
Accepted: 2016-12-20

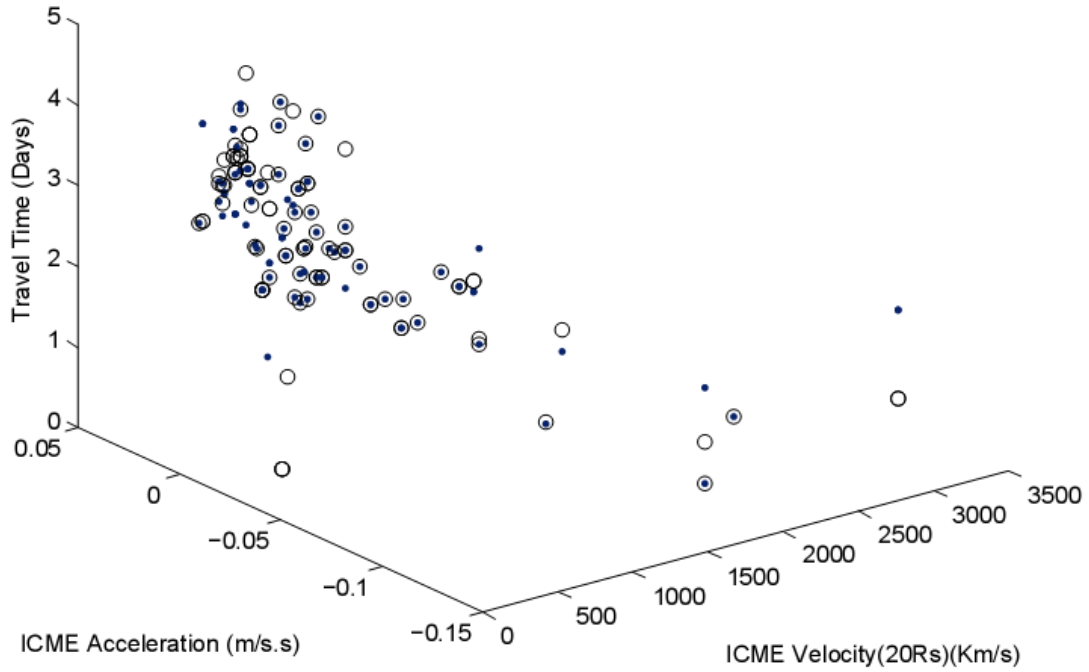

Figure 3: The dependence of the ICME velocities and accelerations on their travel time from the Sun to the Earth, (Upper): for the initial ICME velocity, (Lower): for ICME velocity at a distance 20 $R_{\odot}$ from the Sun.

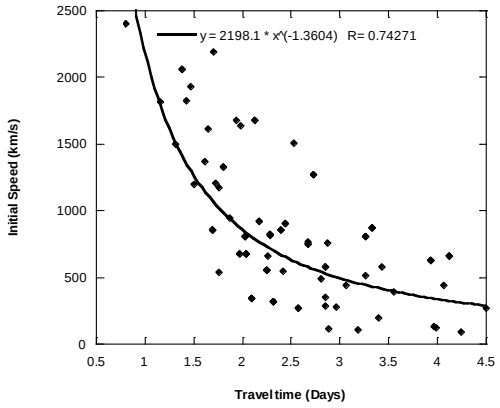

Figure 4: The relationship between calculated ICME travel time and initial speed.

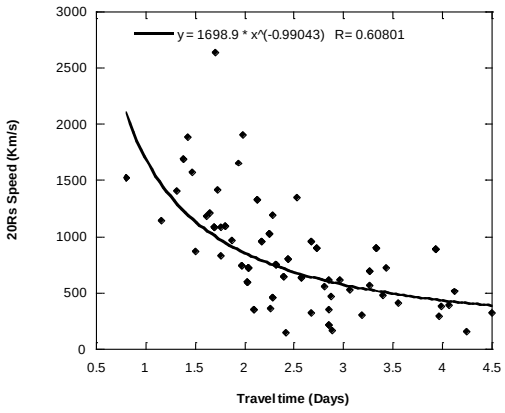

Figure 5: The relationship between calculated ICME travel time and 20Rs speed.

Journal of. Modern Trends in Physics Research
Online ISSN 2636-4220
DOI: 10.19138/mtpr/(16)1-10
Accepted: 2016-12-20

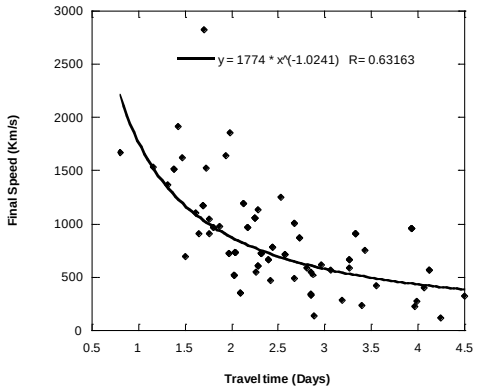

Figure 6: The relationship between calculated ICME travel time and final speed.

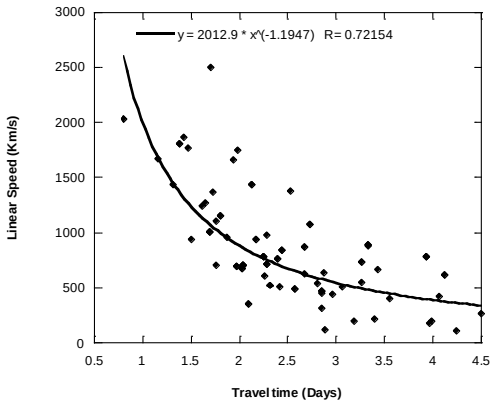

Figure 7: The relationship between calculated ICME travel time and linear speed.

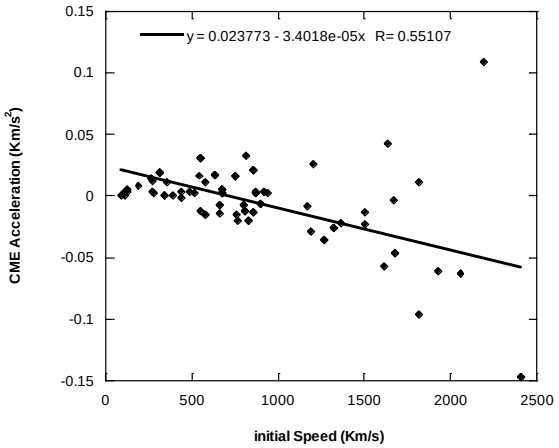

Figure 8: The relationship between initial speed and acceleration of ICMEs.

6. CONCLUSION

We propose a deep ANN approach to detect and list ICMEs using ANN to get the same list tabulated by Cane and Richardson. We trained our ANN application to detect signatures of ICME tabulated by Cane and Richardson during the solar period 1996-2007. Using our ANN application, we succeeded to match 97 % of the listed CME-ICME events created by Cane and Richardson, when we used the initial velocity of the ICME event. While, using the ICME velocity at a distance $20R_{\odot}$, our model succeeded to match only 84 % of the listed ICME events.

The prediction of CME travel time correlated to initial speed of CMEs. We found high correlation coefficient between initial speed of CME and calculated travel time under our model ($R \approx 74$) with power fitting. The prediction of ICME arrival time can be better estimated from initial speed and linear speed of CMEs more than final speed and speed at $20R_{\odot}$.

Journal of. Modern Trends in Physics Research
Online ISSN 2636-4220
DOI: 10.19138/mtpr/(16)1-10
Accepted: 2016-12-20

ACKNOWLEDGMENT

This research is finished by our research team at Space Weather Monitoring Center (SWMC). This work is presented in the 2nd Arab Conference on Astronomy and Geophysics (ACAG-2) at Cairo University on 10/2010 [Mawad *et al.* (2010)], and MTPR-16 International Conference that took place at Cairo University on 20 to 24 April 2019. Authors would like to thank center' director (Prof. Ayman Mahrouh) and research team for supporting this research.

REFERENCES

ASCE Task Committee on Application of Artificial Neural Networks in Hydrology, "Artificial Neural Networks in Hydrology", *Journal of Hydrologic Engineering, parts I and II ASCE*, **5** (2), pp. 115-137, 2000.

Baum, E.; Haussler, D.; "What size net gives valid generalization?", *Neural Computation* **1**, pp. 151-160, 1989.

Bhat, P. (Fermi National Accelerator Lab., Batavia, IL (USA)); Loennblad, L. (Lund Univ. (Sweden). Dept. of Theoretical Physics); Sugano, Katsuhito (Argonne National Lab., IL (USA)); Meier, K.; Deutsches Elektronen-Synchrotron (DESY), Hamburg (Germany, F.R.), "Using neural networks to identify jets in hadron-hadron collisions", Proceeding of The Summer Study on HEP, Research Directions-the Decade, Snowmass, Colorado, 1990.

Bourquin.J., Schmidli. H., Van Hoogevest. P., and Leuenberger.H, "Application of Artificial Neural Networks (ANN) in the Development of Solid Dosage Forms," *Pharm. Dev. Technol.* **2** pp.111-121 (1997).

Burlaga, L., E. Sittler, F. Mariani, R. Schwenn: Magnetic loop behind an interplanetary shock – Voyager, Helios, and IMP 8 observations, *J. Geophys. Res.*, **86** (1981), pp. 6673-6684, Google Scholar, DOI: 10.1029/JA086iA08p06673.

Cane, H. V.; Richardson, I. G.; von Rosenvinge, T. T.: 2010, A study of solar energetic particle events of 1997-2006: Their composition and associations, *Journal of Geophysical Research*, Volume **115**, Issue A8, CiteID A08101, ADS: 2010JGRA..115.8101C, DOI: 10.1029/2009JA014848.

Cargill, P. J.; Schmidt, J. M.: 2002, Modelling interplanetary CMEs using magnetohydrodynamic simulations, *Annales Geophysicae*, vol. **20**, Issue 7, pp.879-890, ADS: 2002AnGeo..20..879C, DOI: 10.5194/angeo-20-879-2002 .

Clausen, L.B.N., S.E. Milan, A. Grocott (2014): Thermospheric density perturbations in response to substorms, *J. Geophys. Res. (Space Phys.)*, **119** (2014), pp. 4441-4455, DOI: 10.1002/2014JA019837 , Google Scholar, URL.

Duperier, A.: 1942, Cosmic Rays and Magnetic Storms, *Nature*, Volume **149**, Issue 3786, pp. 579-580 (1942). ADS: 1942Natur.149..579D, DOI: 10.1038/149579a0.

Forbush, S. E.: 1938, On cosmic-ray effects associated with magnetic storms, *Terrestrial Magnetism and Atmospheric Electricity*, Volume **43**, Issue 3, p. 203, ADS: 1938TeMAE..43..203F, DOI: 10.1029/TE043i003p00203.

Gardner, L., J.J. Sojka, R.W. Schunk, R. Heelis: 2012, Changes in thermospheric temperature induced by high-speed solar wind streams, *J. Geophys. Res. (Space Phys.)*, **117** (2012), p. A12303, DOI: 10.1029/2012JA017892, Google Scholar, URL.

Gopalswamy N.; Lara A.; Lepping R. P.; Kaiser M. L.; Berdichevsky D.; CYR O. C. S., Interplanetary acceleration of coronal mass ejections, *Geophysical research letters*, vol. **27**, 2000.

Gopalswamy, N; Lara, A; Yashiro, S; Kaiser, M.; Howard, Russell A., Predicting the 1-AU arrival times of coronal mass ejections, *Journal of Geophysical Research*, vol. **106**, Issue A12, p. 29207-29218, 2001.

Gosling, J. T.; Skoug, R. M.; McComas, D. J.; Smith, C. W.: 2005, Direct evidence for magnetic reconnection in the solar wind near 1 AU, *Journal of Geophysical Research: Space Physics*, Volume **110**, Issue A1, CiteID A01107. ADS: 2005JGRA..110.1107G, DOI: 10.1029/2004JA010809.

Hagan, M. T. and Benhaj, M.; Training feed-forward networks with the Narquardt algorithm, IEEE Transaction on Neural Networks, pp. 861-867, 1994.

Hamid, A. K., Scatterings from spherical shell with a circular aperture using neural networks approach, *Canadian Journal of Physics*, vol. **76**, pp. 63-67, 1998.

Hidalgo, M.A. , T. Nieves-Chinchilla, J.J. Blanco (2013): On the flux-rope topology of ejecta observed in the period 1997–2006, Sol. Phys., **284** (2013), pp. 151-166, DOI: 10.1007/s11207-012-0191-6, Scopus, Google Scholar, URL.

Klein, L. W.; Burlaga, L. F., Interplanetary magnetic clouds at 1 AU, *Journal of Geophysical Research*, vol. **87**, Feb. 1, 1982, p. 613-624.
L. Gardner, J.J. Sojka, R.W. Schunk, R. Heelis

Lepping, R. P.; Burlaga, L. F and Jones, J. A., Magnetic field structure of interplanetary magnetic clouds at 1 AU, *Journal of Geophysical Research* (ISSN 0148-0227), vol. **95**, Aug. 1, 1990, p. 11957-11965.

Looney, C. G.; Advances in feed-forward neural networks: demystifying knowledge acquiring black boxes, *IEEE Transaction on Knowledge Data Engineering* **8**, pp. 211-226, 1996.

Low, B.C. (2001): Coronal mass ejections, magnetic flux ropes, and solar magnetism, *J. Geophys. Res.*, **106** (2001), pp. 25141-25164, DOI: 10.1029/2000JA004015, Scopus, Google Scholar, URL.

Mawad, Ramy; (2015): On the correlation between Earth's orbital perturbations and oscillations of sea level and concentration of greenhouse gases, *J. Modern Trends in Phys. R.*, Vol. **15** (MTPR-14) pp. 1-9.
Bibcode: 2015ElSS...8031067F. URL.

Mawad, Ramy; Farid, Hussien M.; Youssef, M.; Yousef, S. (2014a): Empirical CME-SSC listing model, *J. Modern Trends in Phys. R.*, Vol. **14** p. 130-136. Bibcode: 2014JMTPR..14..130M . https://doi.org/10.19138/mtpr/(14)130-136

Mawad, Ramy; M. Yousef, A. Radi, A. Mahrous (2010): The Prediction of the interplanetary Coronal Mass Ejection using Neural Networks; The 2nd Arab Conference on Astronomy and Geophysics (ACAG-2); 10/2010.

Mawad, Ramy; Mosalam Shaltout (2011). Empirical Model of the Travel Time of Interplanetary Coronal Mass Ejection Shocks. *NRIAG Journal of Astronomy and Astrophysics*, Special Issue, **5**, PP. 47-61.

Mawad, Ramy; Youssef, Mohamed; Yousef, Shahinaz M.; Abdel-Sattar, Walid (2014b), Quantizated variability of Earth's magnetopause distance, *J. Modern Trends in Phys. R.*, Vol. **14** p. 105-110. Bibcode: 2014JMTPR..14..105M. https://doi.org/10.19138/mtpr/(14)105-110 .

McKenna-Lawlor, S. M. P.; Dryer, M.; Smith, Z.; Kecskemety, K.; Fry, C. D.; Sun, W.; Deehr, C. S.; Berdichevsky, D.; Kudela, K.; Zastenker, G.: 2002, Arrival times of Flare/Halo CME associated shocks at the Earth: comparison of the predictions of three numerical models with these observations, *Annales Geophysicae*, vol. **20**, Issue 7, pp.917-935. ADS: 2002AnGeo..20..917M, DOI: 10.5194/ANGEO-20-917-2002.

Michałek, G.; Gopalswamy, N.; Lara, A.; Manoharan, P. K.: 2004, Arrival time of halo coronal mass ejections in the vicinity of the Earth, *Astronomy and Astrophysics*, v.**423**, p.729-736 (2004), ADS: 2004A&A...423..729M , DOI: 10.1051/0004-6361:20047184.

Owens, M., P. Cargill: 2004, Predictions of the arrival time of Coronal Mass Ejections at 1 AU: an analysis of the causes of errors, *Annales Geophysicae* (2004) **22**: 661–671.

Richardson and Cane, Near-Earth Interplanetary Coronal Mass Ejections during Solar Cycle 23 (1996--2009): 2010, Catalog and Summary of Properties, *Solar Physics*, June 2010, Volume **264**, Issue 1, pp 189–237 (2010).

Richardson, Farrugia and Cane, A statistical study of the behavior of the electron temperature in ejecta, *JGR* (1997).

Richardson, I.G., H.V. Cane (2011): Galactic cosmic ray intensity response to interplanetary coronal mass ejections/magnetic clouds in 1995–2009, *Sol. Phys.*, **270** (2011), pp. 609-627, DOI: 10.1007/s11207-011-9774-x, Scopus, Google Scholar, URL.

Richardson, Ian; Cane, Hilary: 2008, Proceedings of the 30th International Cosmic Ray Conference. July 3 - 11, 2007, Mérida, Yucatán, Mexico. Edited by Rogelio Caballero, Juan Carlos D'Olivo, Gustavo Medina-Tanco, Lukas Nellen, Federico A. Sánchez, José F. Valdés-Galicia. Universidad Nacional Autónoma de México, Mexico City, Mexico, 2008. Volume 1, p.319-322. ADS: 2008ICRC....1..319R .

Shaltout, Mosalam; Ayman Mahrous, Mohamed Youssef, Ramy Mawad (2008). Determination of the arrival time of ICME Shock to Earth's Magnetosphere. *NRIAG Journal of Astronomy and Geophysics*; pp. 28-24.
URL.

Vandegriff, Jon; Wagstaff, Kiri; Ho, George; Plauger, Janice; Forecasting space weather: Predicting interplanetary shocks using neural networks, Advances in Space Research 36 (2005) 2323–2327, 2005.

Whang, Y. C.; Burlaga, L. F., The coalescence of two merged interaction regions between 6.2 and 9.5 AU - September 1979 event, Journal of Geophysical Research (ISSN 0148-0227), vol. 91, Dec. 1, 1986, p. 13341-13348.

Wimmer-Schweingruber, R. F. , N. U. Crooker, Andre Balogh, Volker Bothmer (2003): Understanding Interplanetary Coronal Mass Ejection Signatures, Space Science Reviews 123(1-3) ·DOI: 10.1007/s11214-006-9017-x.

Zhang, J., I.G. Richardson, D.F. Webb, N. Gopalswamy, E. Huttunen, J.C. Kasper, N.V. Nitta, W. Poomvises, B.J. Thompson, C.C. Wu, S. Yashiro, A.N. Zhukov, Solar and interplanetary sources of major geomagnetic storms (Dst ≤−100 nT) during 1996–2005, *J. Geophys. Res. (Space Phys.)*, **112** (2007), p. A10102, DOI: 10.1029/2007JA012321, Google Scholar, URL.

Zurbuchen, Thomas H, Richardson, I. G. (2006): In-Situ Solar Wind and Magnetic Field Signatures of Interplanetary Coronal Mass Ejections, Space Science Reviews 123(1-3). DOI: 10.1007/s11214-006-9010-4.